Nat. Hazards Earth Syst. Sci. Discuss., 3, 2379–2417, 2015
www.nat-hazards-earth-syst-sci-discuss.net/3/2379/2015/
doi:10.5194/nhessd-3-2379-2015

Natural Hazards and Earth System Sciences Discussions
Open Access

The importance of erosion for debris flow runout modelling from applications to the Swiss Alps

F. Frank[1], B. W. McArdell[1], C. Huggel[2], and A. Vieli[2]

[1]Swiss Federal Institute for Forest, Snow and Landscape Research WSL, Birmensdorf, Switzerland
[2]Department of Geography, University of Zurich-Irchel, Zurich, Switzerland

Received: 9 March 2015 – Accepted: 11 March 2015 – Published: 10 April 2015

Correspondence to: B. W. McArdell (brian.mcardell@wsl.ch)

Published by Copernicus Publications on behalf of the European Geosciences Union.

Abstract

This study describes an investigation of channel-bed erosion of sediment by debris flows. An erosion model, developed using field data from debris flows at the Illgraben catchment, Switzerland, was incorporated into the existing RAMMS debris-flow model, which solves the 2-D shallow-water equations for granular flows. In the erosion model, the relationship between maximum shear stress and measured erosion is used to determine the maximum potential erosion depth. Additionally, the maximum rate of erosion, measured at the same field site, is used to constrain the erosion rate. The model predicts plausible erosion values in comparison with field data from highly erosive debris flow events at the Spreitgraben torrent channel, Switzerland in 2010, without any adjustment to the coefficients in the erosion model. We find that by including channel erosion in runout models a more realistic flow pattern is produced than in simulations where entrainment is not included. In detail, simulations without channel bed erosion show more lateral outflow from the channel where it has not been observed in the field. Therefore the erosion model may be especially useful for practical applications such as hazard analysis and mapping, as well as scientific case studies of erosive debris flows.

1 Introduction

Debris flows in mountain areas are one of the most important landscape forming processes in high alpine catchments. Numerous debris fans as well as larger and flat-angled alluvial fans were constructed at least partly by debris flows, mostly after the deglaciation at the beginning of Holocene (Kober et al., 2012). In recent decades, previously stable sediment deposits or rock walls became destabilized in the Swiss Alps (Huggel et al., 2011; Tobler et al., 2014). As a consequence, relatively large debris flow events occurred. The problem has become worse due to increased sediment input connected to intense rainfall activity (e.g. Tobler et al., 2014) or in some cases snowmelt

NHESSD
3, 2379–2417, 2015

activity in early summer (e.g. Graf et al., 2011) which can readily mobilize the debris. The recent large debris flows are unusual in that they have caused unprecedented amounts of erosion on the debris fans or alluvial fans, thereby increasing awareness of the importance of debris-flow erosion, especially for practical applications such as runout analysis and hazard mapping (e.g. Rickenmann and Zimmermann, 1993; Kienholz et al., 2010).

Runout models are an increasingly applied tool to reconstruct previous events and simulate scenarios of debris flow events for research and practical application. One challenge with the application of runout models for hazard analysis is that the initial volume of the debris flow entering a reach, e.g. at the upstream end of a modelling project site, is often substantially smaller than the volume of the debris flow leaving the reach, due to erosion of sediment from the channel bed along the channel.

In current debris flow runout models without erosion, to achieve the design volume for the lowermost object of interest along a torrent channel (e.g. a village on the lower fan), it is necessary to start the model with all of the debris flow volume at the upstream end. This may result in an over-prediction of debris flow discharge and flow depth at the upstream end of the channel, especially if channel erosion occurs. In places where the modelled discharge is large, compared to the channel capacity, overflow results. The loss of a considerable portion of modelled material due to lateral overflow and overbank deposition can even lead to an under-prediction of the runout distance. On the contrary, when implementing the observed initial volume at the upstream end, a runout model without entrainment tends to under-predict the runout patterns. Both approaches could therefore lead to unrealistic hazard assessments. A runout model including entrainment can potentially improve the quality of the prediction of observed flow patterns by improving the accuracy of the prediction of flow depth and discharge along the flow path due to the entrainment of sediment and the increase in volume and peak discharge of a debris flow.

Recent debris flow research mainly focused on the bulk properties and the physical behavior of the debris flow process itself (e.g. Iverson 1997; McArdell et al., 2007;

NHESSD
3, 2379–2417, 2015

Jakob and Hungr, 2005). Physically-based numerical models were developed to investigate runout distance and inundation patterns as well as flow heights and flow velocities (Crosta et al., 2003; D'Ambrosio et al., 2003; Medina et al., 2008; Hungr and McDougall, 2009; Christen et al., 2012). Only recently have researchers focused on better understanding the process by which debris flows entrain sediment from the bed of a torrent channel as part of the erosion process (e.g. Hungr et al., 2005; Mangeney et al., 2007; Berger et al., 2011; Iverson et al., 2011; McCoy et al., 2010, 2012 and 2013).

Debris flow entrainment modelling has been introduced into runout models using algorithms considering the properties of the debris flow (Crosta et al., 2003; D'Ambrosio et al., 2003; Medina et al., 2008). Another approach relies on user-specified erosion layer properties (Beguería et al., 2009; Hungr and McDougall, 2009; Hussin et al., 2012) where the user predefines the volume or depth of eroded sediment. An example for this model type was implemented by Hussin et al. (2012) within the RAMMS 2-D debris flow runout model (Christen et al., 2012). Hussin et al. (2012) used a predefined entrainment method including one or more erosion layers with an absolute thickness specified by the model user wherein an erosion layer is instantaneously eroded when a user-specified critical shear stress is exceeded. This approach is based on the work of Sovilla et al. (2006) for describing the entrainment of snow by avalanches. However, in these modelling approaches the user often must pre-specify the thickness of the erodible layer.

Field observations of the entrainment of sediment from torrent channel beds are rather rare. Rickenmann et al. (2003) studied debris-flow erosion in field and laboratory experiments. They concluded that the fragmentation of material from a matrix (gravel bed or bedrock) depends on the exposure of the particle to the basal forces acting on the matrix, and furthermore that the removal of sediment increases with increasing water content. To assess the timing and the absolute erosion depth caused by natural debris flows at the Illgraben channel, Berger et al. (2010a, 2011) installed a novel channel bed erosion sensor based on the concept of an electrical resistance chain.

McCoy et al. (2013) recently studied basal forces generated by erosive debris flows in Chalk Cliff catchment, Denver, Colorado USA, using a similar type of instrumentation consisting of erosion sensors similar to those in the Illgraben as well as erosion bolts in bedrock and a small force plate. They concluded that debris flows in the field show much broader distributions of basal force than in the laboratory, which they attributed to wider grain size distributions observed in the field. Laboratory results are, in any case, difficult to apply for investigating debris-flow erosion due to problems arising when scaling small-scale laboratory results to the field (e.g. Iverson and Denlinger, 2001; Rickenmann et al., 2003; Reid et al., 2011; McCoy et al., 2013).

The goal of this paper is to demonstrate the importance of debris-flow erosion for runout modelling, which could be used for hazard assessment. To achieve this goal, we developed and implemented an erosion model within a debris-flow runout model and use it as a tool to assess the potential importance of debris-flow erosion. Future, potential applications include both post-event analysis and hazard analysis for future events.

2 The erosion model development site: Illgraben catchment, Switzerland

The catchment of the Illgraben torrent is located in Southern Switzerland, in Canton Valais (Fig. 1a) and has an area of overall 10.9 km^2 (Fig. 1b). The Vanoischi sub-catchment (Fig. 1b) produces several debris flows every year and covers only 4.6 km^2. The geology of the sediment-delivering north-facing wall below the Illhorn mountain (2717 m a.s.l.) is comprised mainly of banded quartzite while the opposite wall consists of dolomites and dolomite breccias which form massive cliffs (Gabus et al., 2008). The north facing side of the catchment is quite heavily exposed to surface erosion processes and frequently delivers sediment into the debris flow initiation zones (Bennet et al., 2012, 2013).

The main debris flow activity at Illgraben is from May through October and is mostly due to convective rainstorms. The resulting runoff mobilizes sediment deposits in steep bedrock channels (Berger et al., 2010b). Because of its high degree of debris-flow activity, this catchment became one of the most studied debris flow sites in the Alps. During the last decade, studies focused on various aspects of the debris flow process addressing the flow process itself (Hürlimann et al., 2003; McArdell et al., 2007), developing a reliable warning system for debris flows based on flow detection (Badoux et al., 2009), studying sediment transfer (Berger et al., 2010b, Bennet et al., 2012, 2013) and the erosion process (Berger et al., 2010a, b, 2011; Schürch et al., 2011a, b; Bennet et al., 2014). Today, the channel is equipped with several measurement installations which allow estimation of typical flow parameters such as front velocity and flow depth. Other debris flow properties are measured using force plates on the channel bed and on a lateral wall to determine basal and lateral stresses as well as bulk density (McArdell et al., 2007; Berger et al., 2011; Schürch et al., 2011b).

3 The erosion model application site: Spreitgraben, Switzerland

The catchment of the Spreitgraben torrent is located in Central Switzerland, near the village of Guttannen at the North side of the Grimselpass in Canton Bern (Fig. 2a). The catchment area is about 4.25 km^2. Foliated gneisses of the Aare massif consisting of crystalline rock dominate the geology. The steep rockwall below the Ritzlihorn (3263 m a.s.l.) is north-east exposed and has steep gullies and couloirs across its entire width. Weathering processes cause frequent sediment supply mostly by rockfall and snow avalanches. The largest activity occurs from spring until mid-summer (April to July) (Geotest, 2010). Daily warming has been observed to cause a considerable increase in rockfall frequency and is thought to be related to snow melting processes during springtime. Furthermore, permafrost degradation above 2700 m a.s.l. was suggested to have contributed to the occurrence of a rock avalanche recorded on 17 July 2009 which deposited about 50 000 m^3 of fresh sediment (Geotest, 2010) at the Schafegg slope on the Ritzlihorn. Consequently, debris flow initiation within these deposits increased in frequency and led to a destabilization of the ice–firn–debris mixture

NHESSD
3, 2379–2417, 2015

below the rock wall in 2010 and more intensively in 2011 (Fig. 2b; Geotest, 2012). During the years 2009–2011 a total volume of more than 600 000 m^3 of sediment were transported into the Hasliaare River (Tobler et al., 2014).

For the active year 2010 at Spreitgraben – when the first two highly erosive debris flows occurred – two LiDAR-based digital terrain models (DTM) are available. They were collected in middle April 2010 and middle of August 2010, and cover the entire active part of the debris flow channel for the debris flow events in 2010 (Table 1).

These 2010 debris flow events extend from the bottom of the Ritzlihorn wall down to the far most reaching debris depositions in the valley Hasliaare River near the village Boden (Fig. 2). For various channel sections, these DTMs allow determination of the elevation changes which occurred during the debris flow season (2010) at the Spreitgraben. The erosion and deposition along the channel is systematically analyzed based on the discretization of the Spreitgraben channel on the fan into 54 bins of similar length (≈ 20 m) along the central flow line. Bins 1 to 54 are located between the former lower firn boundary (1310 m a.s.l.) of the Inner Spreitgraben (July 2009) and the gallery of the Grimselpass road just above the confluence (940 m a.s.l.) into the Hasliaare Valley (Fig. 2c). The erosion observed within the bins is the net bed level change and the erosion volume per bin area [$m^3\,m^{-2}$] yields the net bed level change (m of vertical erosion) within each bin (Sect. 5).

4 Debris-flow erosion modelling method

The RAMMS debris-flow runout model (rapid mass movement system) was selected for this project because it is in development at the Swiss Federal Institute for Forest, Snow and Landscape Research WSL, and because RAMMS is already a widely used model for practical as well as scientific debris flow applications. However, it would be possible to incorporate the erosion algorithm into other debris flow runout models.

To investigate the importance of debris-flow erosion on the runout of debris flows, we modified the RAMMS runout model to include a field-data-based algorithm to describe the incorporation of channel-bed sediment into a debris flow. First we describe the governing equations of the runout model, and then we describe the development of the erosion algorithm. The erosion algorithm is empirical and based on field data (Berger et al., 2011; Schürch et al., 2011b), and it describes the potential erosion depth as a function of the basal shear stress produced by the debris flow. Because it is empirical, it has to be applied with caution to other field sites.

Finally, the model is applied and evaluated at the example of two large debris flow events from Spreitgraben, Switzerland.

4.1 Computational debris-flow model RAMMS

The RAMMS debris-flow model uses the 2-D depth-averaged shallow water equations for granular flows in three dimensions given by the coordinates of the topographic surface of the digital elevation model in a Cartesian coordinate system (x,y,z) and at time (t) (Bartelt et al., 1999; Christen et al., 2010). The mass balance equation incorporating the field variables flow height $H(x,y,t)$ and flow velocity $U(x,y,t)$ is given by

$$\dot{Q}(x,y,t) = \partial_t H + \partial_x (HU_x) + \partial_y (HU_y), \tag{1}$$

where $\dot{Q}(x,y,t)$ denotes the mass production source term and U_x and U_y are the depth-averaged velocities in horizontal directions x and y (Christen et al., 2010). The conservation of momentum in two directions x and y is given by the depth-averaged momentum balance equations:

$$S_{g_x} - S_{f_x} = \partial_t (HU_x) + \partial_x \left(c_x H U_x^2 + g_z k_{a/p} \frac{H^2}{2} \right) + \partial_y (HU_x U_y), \tag{2}$$

$$S_{g_y} - S_{f_y} = \partial_t (HU_y) + \partial_x (HU_x U_y) + \partial_y \left(c_y H U_y^2 + g_z k_{a/p} \frac{H^2}{2} \right), \tag{3}$$

where the earth pressure coefficient $k_{a/p}$ is normally set to 1 when using the standard Voellmy–Salm friction approach, c_x and c_y are topographical coefficients determined

NHESSD
3, 2379–2417, 2015

from the digital elevation model, S_g represents the effective gravitational acceleration, and S_f the frictional deceleration in directions x and y (Christen et al., 2010). The frictional deceleration S_f of the flow is calculated using the Voellmy friction relation (Salm et al., 1990, 1993) and describes the Coulomb friction μ scaling with the normal stress and the turbulent friction ξ depending on the velocity squared (Christen et al., 2012; Bartelt et al., 2013):

$$S_f = \mu \times \rho \times \mathrm{H}g\cos(\phi) + \frac{(\rho)gU^2}{\xi} \tag{4}$$

where ρ is the mass density, g is the gravitational acceleration, ϕ is the slope angle, and $\mathrm{H}g\cos(\phi)$ is the normal stress on the surface it is over-running. The tangent of the effective internal friction angle of the flow material can be specified for the resistance of the solid phase (the term containing μ) which dominates deceleration behavior. In contrast, the resistance of the viscous or turbulent fluid phase (the term including ξ) prevails when the flow is moving quickly (Bartelt et al., 2013).

Bartelt et al. (2013) propose a comprehensive method for calibrating the RAMMS debris flow runout model starting with the collection of model input data from a previous event (debris flow volume, discharge hydrograph) and field data which is useful for the calibration of the model (runout pattern, runout distances, flow heights, flow velocities). Secondly, the RAMMS model can be applied by selecting plausible friction parameters (ξ and μ) considering the results of recent model applications and the field data of the study. The final step is to do a comparative analysis of the model outputs and the field data, especially runout pattern data such as runout distance and lateral overflow, front flow travel time and flow heights. The final calibration of the model input parameters can be established using an iterative approach.

The main challenge is to calibrate the runout model using field data varying from event to event. Further corroboration of the simulation results with comprehensive data will increase the confidence in the model results and the parameters used (Christen et al., 2012; Bartelt et al., 2013). The RAMMS debris-flow model is currently in use for practical applications (e.g. Scheuner et al., 2011) as well as for scientific purposes (Hussin et al., 2012).

4.2 Debris-flow erosion model

The erosion modelling approach outlined in this study is based on field data from the Illgraben catchment in Switzerland. The erosion model consists of two components, where the potential erosion depth is predicted as a function of channel-bed shear stress, and the maximum vertical rate of channel-bed sediment erosion is constrained by other field observations. Figure 3 illustrates the plausibility of this approach based on the field data from the Illgraben and Spreitgraben catchments.

The erosion data set from Illgraben used as the basis for the model consists of differential elevation models based on pre- and post-event DTMs and an analysis of the depth of net erosion in a cell as a function of the estimate of local shear stress at the Illgraben debris-flow catchment (Schürch et al., 2011b). Corresponding flow heights were estimated by Schürch et al. (2011b) using interpolated values between lateral levées of the event. The shear stress τ that is present at a given point at the base of the flow and acting on the channel bed is given by the depth-slope product:

$$\tau = \rho \times g \times h \times \phi, \tag{5}$$

where ρ is the bulk mass density of the flow, h is flow height, and ϕ is channel slope. Following the 50 % percentile line describing the distribution of elevation change measured for four debris flow events at the Illgraben (Fig. 3a in Schürch et al., 2011b) we can approximate the average potential erosion depth at the Illgraben as a linear function of shear stress with the proportionality factor $\frac{dz}{d\tau} = 0.1\,\mathrm{m\,kPa^{-1}}$.

In the RAMMS model, the erosion algorithm is defined by the maximum potential erosion depth e_m and the maximum erosion rate. A linear relationship between maximum shear stress observed and the erosion measured by Schürch et al. (2011b) is used to determine the maximum potential erosion depth (Eq. 6). It is calculated using

NHESSD
3, 2379–2417, 2015

a critical shear stress $\tau_c = 1\,\mathrm{kPa}$ and an average potential erosion depth as a function of basal shear stress:

$$e_m = \begin{cases} 0 \text{ for } \tau < 1\,\mathrm{kPa} \\ -\frac{dz}{d\tau}(\tau - \tau_c) \text{ for } \tau \geq 1\,\mathrm{kPa} \text{ and } \frac{dz}{dt} \leq 0.25\,\mathrm{m\,s^{-1}} \end{cases} \quad (6)$$

In addition, an estimated maximum erosion rate based on values measured at the erosion sensor site during the Illgraben debris flow event of 1 July 2008 (Berger et al., 2011) is used to define the upper limit for erosion rates, $\frac{dz}{dt} \leq 0.25\,\mathrm{m\,s^{-1}}$.

This limit prevents the model from entraining all of the potentially-available sediment within only one time step. Such rapid entrainment is unrealistic and would result in unrealistically large peak flow discharges. This erosion rate is consistent with other field observations. From large-scale debris-flow erosion experiments at the USGS debris flow flume, Reid et al. (2011) reported erosion rates ranging from 0.05 to $0.10\,\mathrm{m\,s^{-1}}$. McCoy et al. (2012) reported a maximum erosion rate of about $0.14\,\mathrm{m\,s^{-1}}$ within the headwaters of a natural debris flow catchment at Chalk Cliffs, Colorado, USA. The maximum erosion rate ($0.25\,\mathrm{m\,s^{-1}}$) implemented in our erosion model is somewhat larger than reported in the other studies, however, the flows at the Illgraben are also larger in size than in the other studies. The erosion rate in the model can be modified by the user if e.g. local field data are available.

Schürch et al. (2011b) noted that field data showed substantial erosion taking place when a basal shear stress of 3–4 kPa was exceeded. However, a linear fit to the 50 % percentile distribution line on Fig. 3a in Schürch et al. (2011b) results in a critical shear stress τ_c of 1 kPa, below which little erosion was observed. While it would be possible to implement a non-linear fit to the data, this was considered to yield only a small improvement. In addition, larger erosion depths as observed at Spreitgraben (3 to 4 m) could not be represented with the erosion model because the percentile distribution lines (Fig. 3a in Schürch et al., 2011b) indicate a flattening out of maximum erosion possible to a somehow lower limit of about 1 to 1.5 m of erosion in depth (which may reflect the structure of that data set rather than a real reduction of the slope of the line). Nevertheless, when addressing erosion modelling of smaller debris flow volumes (some 100 to 1000 m^3) in small channels on lower-slope fans (slope < 10°), it may be necessary or desirable to adjust the critical shear stress threshold for erosion, especially if additional data are available.

The probability of erosion used as the basis for this model does not differentiate between cells where little erosion is expected (e.g. the inside bends of a channel bend) or where significant erosion can be expected (e.g. the outside of channel bends, or the channel thalweg). Additionally, it is likely that local shear stress in the field was different than the values determined by Schürch et al. (2011), because the assumptions used to estimate the shear stress are simplifications. In real debris flows, the surface of the flow is typically convex-up in the lateral direction (so the depth in the shear stress estimate should be somewhat larger than the straight-profile assumption made by Schürch et al., 2011), and the local slope of the debris flow surface at the flow front is perhaps different than the slope-parallel surface assumed here. Additionally, bank collapse, knick-point migration, and other processes may influence the failure and erosion of the channel bed at any given location.

The RAMMS model predicts channel-bed erosion, however it does not modify the DTM during the simulation. After each model run, it is possible to subtract the predicted erosion depth from the DTM within the user interface of the RAMMS model, thereby permitting the simulation of complicated multi-event scenarios on e.g. the development of topography.

As a model run progresses, the potential erosion depth (as a function of shear stress) is used to set the maximum erosion depth for each grid point in the model, and the sediment in the channel bed is entrained at specified rate until the potential erosion depth is reached. If the shear stress during an event again exceeds the critical value, then the maximum potential erosion depth (referenced to the bed surface before the simulation) is updated and the channel bed can continue to erode. The model only describes vertical incision and does not consider lateral bank failure as the channel

NHESSD
3, 2379–2417, 2015

Title Page
Abstract Introduction
Conclusions References
Tables Figures
◀◀ ▶▶
◀ ▶
Back Close
Full Screen / Esc
Printer-friendly Version
Interactive Discussion

is deepened. Hence, secondary processes such as bank collapse and the resulting deposition of sediment in the channel are not computed within the model.

Instead, the user can specify polygons where the maximum erosion depth in each polygon can be set to a constant value to allow for simulation of flow directly over open bedrock or engineering structures as well as over channel beds covered by sediments at a known depth. Finally, the coefficients in the model (critical shear stress τ_c, average potential erosion depth per basal shear stress $\frac{dz}{d\tau}$, erosion rate $\frac{dz}{dt}$) can be adjusted if necessary or if better data become available. However because the main goal of this paper is to investigate the importance of erosion, we leave these values at their default settings.

4.3 Erosion model consistency check at Illgraben, Switzerland

The debris flow event of the 1 July 2008 at Illgraben was chosen to test whether the implemented erosion model (Fig. 3, Eq. 6) based on data mostly collected on the upper fan (Fig. 1d) also functions as expected at the lower fan between check dam 27 and 29 (Fig. 1c). The default model values (Eq. 6) describing the erosion behavior are compared to the observations at check dam 29 as well as to the erosion ranges at the erosion sensor site (Berger et al., 2011).

The total event volume of the debris flow on 1 July 2008 was estimated to be $V \approx 58\,000\,\mathrm{m}^3$. The event lasted about 1 h including several secondary surges. Flow parameters measured at the debris flow observation station on check dam 29 are summarized in Table 2.

To verify that the erosion model performs in a reasonable manner when implemented in RAMMS, the model was applied to the reach where erosion rates were measured by Berger et al. (2011) (Fig. 1c). The model was started using an input hydrograph implemented just above check dam 27 (Fig. 1c). The hydrograph data measured at check dam 29 (about 465 m downstream) were used for calibration in which the friction coefficients μ and ξ (Eq. 4) were systematically adjusted until both the travel time and flow depth are similar to the observed values. The best-fit parameters were found to be $\mu = 0.05$ and $\xi = 1200\,\mathrm{m\,s^{-2}}$, and the predicted erosion rates are realistic (Table 2).

After calibration of the friction coefficients – which has to be done when using the Voellmy friction relation in every case, even without erosion – it is clear that the model is capable of re-producing the erosion values observed at the Illgraben channel. This is not surprising, given that the erosion model was derived from field data at the Illgraben, however the relation to define the maximum depth of erosion (Eq. 6) was derived from about 1500 m upstream of the main observation site, where the flow velocity can only be roughly constrained. This suggests that the generalization of the erosion model to define the maximum erosion depth as a function of shear stress may be reasonable, although Berger et al. (2011) argued that pressure fluctuations in the flow, which may be a function of shear stress, could be a physically more realistic way to describe the erosion process. However more work need to be done to develop an erosion model based on pressure fluctuations (Deubelbeiss et al., 2011) and that topic is beyond the scope of this paper.

5 Erosion model application results at Spreitgraben, Switzerland

5.1 Erosion model application setup

The main purpose of the erosion model application at Spreitgraben is to evaluate how the model performs under these very different boundary conditions such as topography (e.g. steeper channel slope) and flow conditions (larger flow heights, discharges and flow volumes). The 2010 debris flow season was chosen for the modelling because the best quality data at the Spreitgraben are available for this year (Fig. 2b, Table 1). Overall, 5 debris flow events were documented in 2010 (Geotest, 2010). The 3 smallest events – each estimated to be $\approx 10\,000\,\mathrm{m^3}$ (Table 1) – were observed to behave more like a debris flood typically characterized by constant flow heights (≈ 0.5 m) over 30 to 60 min (Geotest, 2010). These 3 small events did not exhibit steep debris flow fronts

NHESSD
3, 2379–2417, 2015

and they did not cause significant erosion in the channel. They are therefore neglected herein.

Only the two relatively large debris flow events of 23 July 2010 ($\approx 90\,000\,\mathrm{m}^3$) and 12 August 2010 ($\approx 130\,000\,\mathrm{m}^3$) were considered. These debris flows caused considerable primary erosion of several meters each (Fig. 3) while leading to secondary erosion processes such as bank collapses (Fig. 8). Comparing the annual debris flow volume of 2010 considering runoff and all deposits in the Aare river between influence of the Spreitgraben and the downstream village of Innertkirchen ($\approx 290\,000\,\mathrm{m}^3$) with the total erosion volume measured ($\approx 180\,000\,\mathrm{m}^3$) we calculated, based on the differential elevation data analysis within the bins (Table 1; Fig. 2c), that the total debris flow volume at the lower firn boundary is $V \approx 110\,000\,\mathrm{m}^3$. This result is consistent with estimates by Geotest (2012) based on sediment input from the rock avalanche, erosion underneath the firn deposits and sediment contribution from lateral channels. The debris flow initiation area was mostly covered by the firn deposits and hence are difficult to assess Geotest (2012). Therefore the estimated annual debris flow volume for 2010 at the lower firn boundary (1310 m a.s.l.) is chosen as the starting point for the modelling.

The annual debris flow volume is then distributed between the two debris flow events (Table 3) proportional to their total event volumes estimated by Geotest AG (2012) (Table 1). The two discharge hydrographs required as model input are derived addressing typical debris flow discharge behavior using a simplified four-point hydrograph (Table 3) and a correlation between debris flow volume V and peak discharge Q_p proposed by Rickenmann et al. (1999):

$$Q_\mathrm{p} = 0.1 \times \mathrm{V}^{5/6}\,[\mathrm{m}^3] \qquad (7)$$

Finally, the erosion model applications are performed using the RAMMS debris flow runout modelling software (version 1.5.01) in which the erosion model was implemented. The Voellmy friction parameters were varied systematically as ξ = 200, 500, 1000, 2000 and μ = 0.20, 0.25, 0.30, 0.35, 0.40 in order to investigate the sensitivity of the model results and to find the best overall fit to the field data.

NHESSD
3, 2379–2417, 2015

5.2 Erosion model application results

The most realistic erosion result was found when the model was calibrated using ξ = 200 and μ = 0.20 resulting in a front travel time ≈ 2 min and 30 s between upper fan and gallery of the main road (Fig. 4). Because the parameters ξ = 500, 1000 and 2000 resulted in front travel times clearly shorter than 2 to 4 min (as observed) while leading at the same time to almost no erosion (∼ −0.5 m along the entire channel reach), they were not considered any further in the model sensitivity analysis.

The modelled mean erosion depth per bin using μ = 0.20 and μ = 0.25 generally underestimate observed mean erosion depths along the entire channel reach. Despite depicting constant underestimation, simulations with μ = 0.20 interestingly result in accurate mean erosion estimates just above the gallery (bins 48 to 54). When chosing μ = 0.25, the model also describes realistic erosion behavior yet the absolute values are one standard diameter less than the observed mean erosion values in the upper channel reach (bins 1 to 20) covering the Inner Spreitgraben reach (Fig. 2) down to the confluence area (bins 20–21) with the Outer Spreitgraben (Fig. 4a).

Modelled mean erosion values per bin using μ = 0.30, μ = 0.35 and μ = 0.40 are mostly located within ± 1 standard deviation of the observed data (Fig. 4a). Using μ = 0.30, we persistently underestimate erosion by approximately one standard deviation (Fig. 4a). Within some short channel reaches (bins 17 to 20 and 38 to 43), the erosion modelling using μ = 0.30 works quite well but overestimates erosion along the smoother channel reach just above the gallery (bins 48 to 54). Simulations using μ = 0.35 result in very similar mean erosion values. This modelling experiment generally shows slightly more erosion and fluctuating values between −2 and −6 m which is mostly within ± 1 standard deviation range of the observed data (Fig. 4a).

Finally, the most realistic spatial erosion pattern is obtained using μ = 0.40. Modelled mean erosion values fluctuate around the observed mean incorporating a large channel reach (bins 5 to 38). Mean observed values are rarely precisely reproduced.

NHESSD
3, 2379–2417, 2015

Nevertheless, these simulations ($\mu = 0.40$) result in an accurate prediction of most of the field data modelled.

The modelled cumulative erosion volumes are somewhat underestimated in comparison with the observed cumulative erosion volumes (Fig. 4b). The corresponding result is also apparent in the modelled flow depths. In the case of $\mu = 0.40$, the cumulative erosion volumes are reasonably well predicted along the upper most channel reach (bins 1 to 15). From bins 15 to ~ 35, the cumulative erosion volumes are slightly overestimated but are still plausible. Downstream from bin 35, the modelled cumulative erosion volumes result in an overestimation of about +25 % of the observed cumulative erosion volumes (≈180 000 m^3). Regarding the overall cumulative erosion volume estimation (all bins), the simulations with $\mu = 0.35$ is closest to the observed cumulative erosion volume (≈170 000 m^3). Using $\mu = 0.35$, the erosion model also behaves well along the middle-range channel reach from the confluence downstream (bin 20 to 33) while a constant underestimation of about ≈5000 to 10 000 m^3 has to be considered. Simulations using $\mu = 0.30$ and $\mu = 0.20$ result in predicted cumulative volumes clearly too low compared to observed values (overall −30 and −70 %, respectively) while their erosion volume allocation behave similar in the upper channel reach (bins 1 to 15). As mentioned above, the erosion model results using coefficient $\mu = 0.25$ show quite accurate behavior of erosion volume accumulation along the upper channel reach (bins 1 to 20) but are 40 % below the observed cumulative erosion. Further downstream, erosion volumes are constantly underestimated resulting in about 55 % lower overall erosion volume.

Considering all the results related to the choice of friction coefficients, one can conclude that erosion behavior cannot be precisely represented using only one Coulomb friction value for the entire area. This may be related to the complex topography (e.g. slope angles) respectively that in reality friction angles are not necessarily constant along the channel. While it would be possible to define different friction values for each reach, such fine-tuning does not seem to be warranted in this case because velocity data for the different reaches are not available.

NHESSD
3, 2379–2417, 2015

NHESSD
3, 2379–2417, 2015

6 Discussion

6.1 Flow properties and runout patterns

One important aspect of this modelling study was to evaluate how including erosion affects the runout modelling of debris flows. This includes the influence on flow properties such as the mean front flow velocity and the change in flow height over time which describes the flow hydrograph. The results show that the incorporation of debris-flow erosion modelling within a runout model can improve the overall prediction of runout.

Using the RAMMS debris flow runout model without erosion modelling, the most plausible modelled flow properties (front travel time and hydrograph shape) can be achieved using Voellmy friction coefficients of $\xi = 200\,\mathrm{m^2\,s^{-1}}$ and $\mu = 0.20$. This calibration was done applying the standard RAMMS debris flow runout model without erosion modelling for the largest debris flow event at Spreitgraben (12 August 2010; Geotest, 2010) which had an estimated volume of 130 000 $\mathrm{m^3}$ (Table 1) with the total volume entering the computational domain at the lower firn boundary (Fig. 2b and c).

The runout erosion model was implemented using a realistic initial flow volume of about 50 000 $\mathrm{m^3}$ at the lower firn boundary which produced similar total flow volumes at the gallery (Table 1; location G in Fig. 5) within ±10 % of the estimated event volume at that location. The resulting maximum flow heights as well as the hydrograph using the erosion modelling approach are similar to the no-erosion modelling and consistent with observed peak flow heights of about 5 to 7 m (Fig. 5b). The comparison of runout modelling with and without erosion modelling shows several differences in runout patterns (Fig. 5). The runout erosion modelling improves the modelled runout pattern by reducing most of the lateral overflow obtained in the no-erosion modelling approach Such lateral bank overflows were not observed in the field, although, some individual smaller rocks were ejected from the debris flow due to the highly turbulent flow behavior (Geotest, 2010).

A comparison of the flow depth through time (often referred to as the hydrograph) for both runout model types (no-erosion vs. erosion) at Spreitgraben also shows substantial differences between the models (Fig. 6). Due to the smaller initial volume and discharge, the erosion model (Fig. 6, red lines) has corresponding smaller maximum flow heights on the upper fan (Fig. 6a) and below the confluence with the Outer Spreitgraben (Fig. 6b) by about 2 to 2.5 m which results in fewer lateral overbank outbreaks (Fig. 5).

The reduction of the lateral overflow area is noticable along the upper channel reach (blue area in Fig. 5b). The two main subsequent outbreaks of ∼ 100 to 1000 m^3 predicted by the no-erosion model at approximately 100 m and again at 200 m below location C (both on the orographic left side) are not present in the runout modelling result (Fig. 5b). In this example, the erosion model provides a clearly more realistic result in comparison with the no-erosion model.

Observed front travel times are not well constrained for the 2010 Spreitgraben events. Estimates range from 2 to 4 min between upper channel (location U) and the gallery (location G) (Geotest, 2010). The two different models produce similar overall travel times, e.g. about 2 min 15 s with the no-erosion model and about 2 min 20 s using the erosion runout model (Fig. 6a compared to Fig. 6c). The corresponding mean front flow velocity from bin 1 to 54 along the central flow line (≈1340 m in April 2010) is ≈ 9.9 ms^{-1} for the no-erosion runout model and ≈9.6 ms^{-1} for the erosion runout model. Estimates of flow velocities from oblique video images gave debris flow front velocities of ≈ 8 ms^{-1} at the flow front and of ≈ 5 ms^{-1} just after the flow front had passed (Geotest, 2010). The maximum modelled flow velocities on the top of the gallery (location G) were found to be ≈ 5.0–8.0 ms^{-1} for the erosion model and ≈ 4.5–7.5 ms^{-1} for the no-erosion model during and shortly after peak discharge and are within the observed range of ≈ 8.0 ± 2 ms^{-1} (Geotest, 2010).

The similar propagations and arrival times of modelled hydrographs indicate that the standard model calibration procedure proposed for the RAMMS debris-flow model without erosion (Bartelt et al., 2013) might be also appropriate for the erosion modelling approach. Therefore, we suggest that the basic calibration process can be enhanced by applying the erosion model while using previously calibrated parameters ξ and μ.

NHESSD
3, 2379–2417, 2015

Nevertheless, more comparisons of no-erosion and erosion model have to be conducted in other catchments to judge the reliability of the suggested enhancement of the model calibration process.

The erosion modelling investigations presented in this paper emphasizes the requirement for an erosion model implemented in debris-flow models to improve flow behavior along the channel and inundation patterns on the fan, especially for highly erosive debris flows.

Berger et al. (2011) suggested that entrainment influences the motion of the debris flow because the entrained sediment has to be accelerated from a state of rest up to the speed of the flow; this could be visible in an additional resistance near the flow front. To include entrainment in a debris-flow model, Hussin et al. (2012) predefined one or more erosion layers with an specified thickness which are fully eroded in their model when exceeding a critical shear stress. They noted that the entrainment method used in their erosion model showed high sensitivity to event volume and flow heights in their study at the Faucon catchment in the Southern French Alps. Their approach can deliver accurate results and improve the runout patterns results when back-calculating a previous well-documented debris-flow event. However, their approach requires pre-determined information about the potential erosion depth (layers) normally not available except for past and well documented events. Therefore, this concept is not directly suitable to assess determine the amount of entrainment for future debris flow surges as required for hazard assessment. This problem can only be addressed by predefined entrainment rates based on physical concepts or entrainment rates measured in laboratories or in the field. For example, Medina et al. (2008) implemented an entrainment model where the erosion process is activated if the shear stress exceeds the resistance at the channel bed using a static as well as a dynamic approach. The dynamic approach uses momentum-driven entrainment rates where the entrained mass has to be accelerated to the mean flow velocity.

The erosion model proposed in this study characterizes the erosion process based on the idea that the maximum depth of erosion (Fig. 3, Eq. 6). is a function of basal

NHESSD
3, 2379–2417, 2015

shear stress (Eq. 4). Hence, the erosion model does not require pre-defined maximum erosion depths. Noticeable differences in modelled runout patterns are expected to emerge for larger flow heights depths, larger volumes, steeper (and less distinctive) channel slopes and larger bulk densities (e.g. characteristic of granular debris flows). By constraining the rate of erosion by field observations of maxiumum rates, we account for the suggestion that natural debris flows show rather different erosion behavior than down-scaled laboratory experiments (Iverson and Denlinger, 2001; Rickenmann et al., 2003; Reid et al., 2011; McCoy et al., 2013). The empirical approach using potential erosion depths observed as well as maximum erosion rates in the field offers the opportunity to estimate the expected amount of debris-flow erosion and its effects on hydrograph propagation and runout. Nevertheless, further model tests are necessary to further corroborate the accuracy of this approach.

6.2 Probability occurrence of erosion depths

The comparison of modelled and observed erosion depths observed using the probability density plot offers another method to compare model results. The probability-density analyses of modelled vs. observed erosion depth is based on all the cells (12.621; 2 m by 2 m) within bins 1 to 54 (Fig. 7). The probablity of occurrence for different erosion depths (discretized into decimeter-scale changes) is calculated for all the parameter combinations considered in the erosion modelling (see also Sect. 5).

The model result closest to the field data is the simulation with $\xi = 200\,\mathrm{m^2\,s^{-1}}$ and $\mu = 0.40$, although there is a trend to under-predict maximum erosion depth and to over-predict the area with lower erosion depths. Part of this discrepancy can be explained by processes other than debris-flow erosion, such as bank collapse and the re-working of sediment within the channel by smaller flood flows. This result is also somewhat different than the best-fit erosion model results regarding runout pattern and lateral over-flow described above, where the most realistic result was achieved using $\xi = 200\,\mathrm{m^2\,s^{-1}}$ and $\mu = 0.20$. A more detailed investigation of the best-fit friction coefficients is not possible at this field site due to the imprecision in the observed flow properties (e.g. travel time over the entire reach) which would be necessary for a more precise model calibration.

In general, the Spreitgraben channel was relatively stable prior to the very large debris flow in 2009, although there is a chronology of small debris flows in the past. The debris flow process itself primarily causes vertical deepening of the channel bed (Fig. 8a). This results in an increase in the height and overall steepness of the channel banks, which failed to lower, more stable friction angles (Fig. 8b), with the sediment stored in the channel. The net result is that the channel becomes wider, and with net removal of sediment in the channel bed (e.g. due to debris flow or flood erosion), there is a net lowering of the channel (Fig. 8c).

Therefore, we suggest that the higher probability of the observed upper-range erosion values more than −6 m (see Fig. 4a) are due to the collapse of lateral banks. In-situ observations of the two larger Spreitgraben debris flow events 2010 showed that such secondary erosion processes were regularly occurring within hours up to several days after the debris flow events. Hence, they are related to but not directly caused by the larger debris flows (Geotest, 2010). Highest erosion values were observed especially along the former banks of the channel on the upper fan where the erosion values measured for 2010 are even larger than along the central flow line (Fig. 2c; bins 1 to 15). This indicates that the bank-collapses are causing at least some portion of the higher probability of large net erosion depths observed (> −6 m). Because there is a lack of knowledge about the exact timing, locations and volumes of these lateral collapses in 2010 (this study started in July 2012), it was impossible to conduct a temporal or quantitative analyses of the collapses. Thus, the lateral bank-collapses (Figs. 2c and 8) and their influence on the net erosion values observed (Fig. 7) remain unquantified.

The discussion above raises the possibility that a geomorphic threshold was exceeded which caused the destabilization of the channel on the debris fan and resulted in the debris fan becoming a source of sediment for large debris flows instead of being a depositional environment. The mechanism is that the channel-bed was first strongly eroded by the first large debris flow. This deepened the channel and resulted in a condition where the over-steepened banks partially collapsed (Fig. 8), greatly increasing the amount of sediment available for transport. Subsequent debris flows could then entrain this sediment, thereby increasing their size and causing more channel-bed erosion. This may have also resulted in considerably higher erosion rates at the Spreitgraben than predicted by the erosion model (Fig. 3, Eq. 6) based on the maximum erosion rates measured at Illgraben (Berger et al., 2011). Although such positive feedback mechanisms are plausible, they are difficult to explicitly test. Regarding the initial channel "re-activation" event in 2009, our estimate is that the shear stress must have exceeded ∼ 5 kPa during the first flow, which is consistent with field observations in 2012 and 2013 where smaller debris-floods with estimated maximum shear stress values of ≈ 4–5 kPa did not cause significant channel-bed erosion.

7 Conclusions

The development, implementation and application of the data-based debris-flow erosion model (Sects. 4 and 5) highlights the importance of erosion for runout modelling. The erosion model is based on the relation between calculated basal shear stress and the net erosion (Schürch et al., 2011b) as well as a maximum erosion rate (Berger et al., 2011) which were both measured at the Illgraben channel. The erosion model was evaluated at the Spreitgraben channel and, without additional calibration other than evaluated by using the standard no-erosion model, the model delivers results which are in agreement with field data regarding channel-outbreak patterns and the depth of erosion. Other parameters such as pressure fluctuations due to particles in the flow impacting the bed could provide a more realistic physical basis to describe erosional behavior. However, the model presented herein may be useful until more physically accurate algorithms become available.

The comparison of two RAMMS runout results, either ignoring or including erosion (Sect. 6) illustrates that incorporated erosion can substantially improve the prediction of spatial runout patterns (Fig. 5) as well as flow propagation (Fig. 6). Nevertheless, more

NHESSD
3, 2379–2417, 2015

sensitivity testing of the erosion model has to be conducted to assess the usefulness of the model to other geometric settings and field conditions (e.g. channel slope and event volume). We suggest that inconsistencies between the observed and modelled net elevation change can partly be explained due to erosion originating from different processes (Fig. 8) such as lateral bank-collapse and due to increased erodibility of correspondent sediment deposits. We conclude that including sediment erosion and the resulting volume growth in debris-flow runout modelling can considerably improve the accuracy of model results.

Acknowledgements. The work of F. Frank is part of the TRAMM project (Triggering of Rapid Mass Movements in Steep Terrain) funded by the ETH Competence Centre Environment and Sustainability. We are grateful to Marc Christen and Lisa Dreier (WSL-SLF Davos) for programming the entrainment module and integrating it into the RAMMS runout model.

References

Badoux, A., Graf, C., Rhyner, J., Kuntner, R., and McArdell, B. W.: A debris flow alarm system for the Alpine Illgraben catchment: design and performance, Nat. Hazards, 49, 517–539, 2009.

Bartelt, P., Salm, B., and Gruber, U.: Calculating dense-snow avalanche runout using a Voellmy-fluid model with active/passive longitudinal straining, J. Glaciol., 45, 242–254, 1999.

Bartelt, P., Buehler, Y., Christen, M., Deubelbeiss, Y., Graf, C., and McArdell, B. W.: RAMMS – rapid mass movement simulation, A modeling system for debris flows in research and practice, user manual v1.5, debris flow, manuscript update: 31 January 2013, WSL Institute for Snow and Avalanche Research SLF, available at: http://ramms.slf.ch/ramms/downloads/RAMMS_DBF_Manual.pdf (last access: 5 March 2015), 2013.

Beguería, S., Van Asch, Th. W. J., Malet, J.-P., and Gröndahl, S.: A GIS-based numerical model for simulating the kinematics of mud and debris flows over complex terrain, Nat. Hazards Earth Syst. Sci., 9, 1897–1909, doi:10.5194/nhess-9-1897-2009, 2009.

Bennett, G. L., Molnar, P., Eisenbeiss, H., and McArdell, B. W.: Erosional power in the Swiss Alps: characterizing slope failure at the head of the Illgraben, Earth Surf. Proc. Land., 37, 1627–1640, 2012.

Bennett, G. L., Molnar, P., McArdell, B. W., Schlunegger, F., and Burlando, P.: Patterns and controls of sediment production and transfer in the Illgraben, Switzerland, Geomorphology, 188, 68–82, 2013.
Bennett, G. L., Molnar, P., McArdell, B. W., and Burlando, P.: A probabilistic sediment cascade model of sediment transfer in the Illgraben, Water Resour. Res., 50, 1225–1244, 2014.
Berger, C., McArdell, B. W., Fritschi, B., and Schlunegger, F.: A novel method for measuring the timing of bed erosion during debris flows and floods, Water Resour. Res., 46, W02502, doi:10.1029/2009WR007993, 2010a.
Berger, C., McArdell, B. W., and Schlunegger, F.: Sediment transfer patterns at the Illgraben catchment, Switzerland: implications for the time scales of debris flow activities, Geomorphology, 125, 421–432, 2010b.
Berger, C., McArdell, B. W., and Schlunegger, F.: Direct measurement of channel erosion by debris flows, Illgraben, Switzerland, J. Geophys. Res., 116, F01002, doi:10.1029/2010JF001722, 2011.
Christen, M., Kowalski, J., and Bartelt, P.: RAMMS: numerical simulation of dense snow avalanches in three-dimensional terrain, Cold Reg. Sci. Technol., 63, 1–14, 2010.
Christen, M., Bühler, Y., Bartelt, P., Leine, R., Glover, J., Schweizer, A., Graf, C., McArdell, B. W., Gerber, W., Deubelbeiss, Y., Feistl, T., and Volkwein, A.: Integral hazard management using a unified software environment: numerical simulation tool "RAMMS" for gravitational natural hazards, in: 12th Congress INTERPRAEVENT, Grenoble – France, Proceedings, Vol. 1, International Research Society INTERPRAEVEN T, edited by: Koboltschnig, G.; Hübl, J., and Braun, J., Klagenfurt, 23–26 April 2012, 77–86, 2012.
Crosta, G. B., Imposimato, S., and Roddeman, D. G.: Numerical modelling of large landslides stability and runout, Nat. Hazards Earth Syst. Sci., 3, 523–538, doi:10.5194/nhess-3-523-2003, 2003.
D'Ambrosio, D., Di Gregorio, S., and Iovine, G.: Simulating debris flows through a hexagonal cellular automata model: SCIDDICA S_{3-hex}, Nat. Hazards Earth Syst. Sci., 3, 545–559, doi:10.5194/nhess-3-545-2003, 2003.
Deubelbeiss, Y. and McArdell, B. W.: Dynamic modelling of debris-flow erosion and deposition with application to the USGS debris flow flume experiments, Geophys. Res. Abstr., 14, EGU 2012, p. 7906, http://www.yolandadeubelbeiss.ch/bilder/abstract_EGU2012.pdf (last access: 5 March 2015), 2012.

Gabus, J. H., Weidmann, M., Bugnon, P.-C., Burri, M., Sartori, M., and Marthaler, M.: Geological map of Sierre, LK 1278, sheet 111, scale 1:25,000, in: Geological Atlas of Switzerland, Swiss Geol. Surv., Bern, Switzerland, 2008.
Geotest AG, Zollikofen BE/CH: Several reports about the debris flow events from 2009 to 2011 at the Spreitgraben catchment, Geotest AG, Zollikofen, Switzerland, 2010–2012.
Graf, C., Deubelbeiss, Y., Bühler, Y., Meier, L., McArdell, B., Christen, M., and Bartelt, P.,: Gefahrenkartierung Mattertal: Grundlagenbeschaffung und numerische Modellierung von Murgängen, in: Graf, C. (Red.): Mattertal – ein Tal in Bewegung, Publikation zur Jahrestagung der Schweizerischen Geomorphologischen Gesellschaft, Eidg. Forschungsanstalt WSL, St. Niklaus, Birmensdorf, 29. Juni – 1. Juli 2011, 85–112, 2013.
Huggel, Ch., Clague, J. J., and Korup, O.: Is climate change responsible for changing landslide activity in high mountains?, Earth Surf. Proc. Land., 37, 77–79, 2011.
Hungr, O. and McDougall, S.: Two numerical models for landslide dynamic analysis, Comput. Geosci., 35, 978–992, 2009.
Hungr, O., McDougall, S., and Bovis, M.: Entrainment of material by debris flows, in: Debris-flow hazards and related phenomena, edited by: Jakob, M. and Hungr, O., Springer, Berlin, New York, 135–158, doi:10.1007/b138657, 2005.
Hürlimann, M., Rickenmann, D., and Graf, C.: Field and monitoring data of debris-flow events in the Swiss Alps, Can. Geotech. J., 40, 161–175, 2003.
Hussin, H. Y., Quan Luna, B., van Westen, C. J., Christen, M., Malet, J.-P., and van Asch, Th. W. J.: Parameterization of a numerical 2-D debris flow model with entrainment: a case study of the Faucon catchment, Southern French Alps, Nat. Hazards Earth Syst. Sci., 12, 3075–3090, doi:10.5194/nhess-12-3075-2012, 2012.
Iverson, R. M.: The physics of debris flows, Rev. Geophys., 35, 245–296, 1997.
Iverson, R. M. and Denlinger, R. P.: Flow of variably fluidized granular masses across three-dimensional terrain: 1. Coulomb mixture theory, J. Geophys. Res., 106, 537–552, 2001.
Iverson, R. M., Reid, M. E., Logan, M., LaHusen, R. G., Godt, J. W., and Griswold, J. G.: Positive feedback and momentum growth during debris-flow entrainment of wet bed sediment, Nat. Geosci., 4, 116–121, doi:10.1038/NGEO1040, 2011.
Jakob, M. and Hungr, O.: Debris-flow hazards and related phenomena, Springer, Berlin, New York, 170 p, 2005.
Kienholz H., Frick E., and Gertsch E.: Assessment tools for mountain torrents: SEDEX and bed load assessment matrix, in: Chen SC (ed) Internationales symposion interpraevent in

the Pacific Rim-Taipei (26–30 April). Internationale Forschungsgesellschaft Interpraevent, Klagenfurt, 245–256, 2010.
Kober, F., Hippe, K., Salcher, B., Ivy-Ochs, S., and Kubik, P. W.: Debris-flow – dependent variation of cosmogenically derived catchment-wide denudation rates, Geology, 40, 935–938, 2012.
Mangeney, A., Bouchut, F., Thomas, N., Vilotte, J. P., and Bristeau, M. O.: Numerical modeling of self-channeling granular flows and of their levee-channel deposits, J. Geophys. Res., 112, F02017, doi:10.1029/2006JF000469, 2007.
McArdell, B. W., Bartelt, P., and Kowalski, J.: Field observations of basal forces and fluid pore pressure in a debris flow, Geophys. Res. Lett., 34, L07406, doi:10.1029/2006GL029183, 2007.
McCoy, S. W., Kean, J. W., Coe, J. A., Staley, D. M., Wasklewicz, T. A., and Tucker, G. E.: Evolution of a natural debris flow: in situ measurements of flow dynamics, video imagery, and terrestrial laser scanning, Geology, 38, 735–738, doi:10.1130/G30928.1, 2010.
McCoy, S. W., Kean, J. W., Coe, J. A., Tucker, G. E., Staley, D. M., and Wasklewicz. T. A.: Sediment entrainment by debris flows: in situ measurements from the headwaters of a steep catchment, J. Geophys. Res., 117, F03016, doi:10.1029/2011JF002278, 2012.
McCoy, S. W., Tucker, G. E., Kean, J. W., and Coe, J. A.: Field measurement of basal forces generated by erosive debris flows, J. Geophys. Res.-Earth, 118, 589–602, doi:10.1002/jgrf.20041, 2013.
Medina, V., Hürlimann, M., and Bateman, A.: Application of FLATModel a 2-D finite volume code, to debris flows in the northeastern part of the Iberian Peninsula, Landslides, 5, 127–142, 2008.
Reid, M. E., Iverson, R. M., Logan, M., LaHusen, R. G., Godt, J. W., and Griswold, J. G.: Entrainment of bed sediment by debris flows: results from large-scale experiments, in: Fifth International Conference on Debris-flow Hazards Mitigation, Mechanics, Prediction and Assessment, edited by: Genevois, R., Hamilton, D. L., and Prestinizi, A., Casa Editrice Universita La Sapienza, Rome, Padua, Italy, 14–17 June 2011, 367–374, 2011.
Rickenmann, D.: Empirical Relationships for Debris Flows, Swiss Federal Institute for Forest, Snow and Landscape Research, CH-8903 Birmensdorf, Nat. Hazards, 19, 47–77, 1999.
Rickenmann, D. and Zimmermann, M.: The 1987 debris flows in Switzerland: documentation and analysis, Geomorphology, 8, 175–189, 1993.

Rickenmann, D., Weber, D., and Stepanov, B.: Erosion by debris flows in field and laboratory experiments, in: Proceedings of the Third International Conference on Debris-Flow Hazard Mitigation: Mechanics, Prediction and Assessment, edited by: Rickenmann, D. and Chen, L. C., Davos, Switzerland, 10–12 September 2003, Milpress, Rotterdam, the Netherlands, 883–894, 2003.
Salm, B., Burkard, A., and Gubler, H.: Berechnung von Fliesslawinen: eine Anleitung für Praktiker mit Beispielen, Mitteilung 47, Eidg. Institut für Schnee- und Lawinenforschung SLF, Davos, Switzerland, 1990.
Salm, B.: Flow transition and runout distances of flowing avalanches, Ann. Glaciol., 18, 221–226, 1993.
Scheuner, Th., Schwab, S., and McArdell, B. W.: Application of a Two-Dimensional Numerical Model in Risk and Hazard Assessment in Switzerland, in: 5th International Conference on Debris-Flow Hazards Mitigation: Mechanics, Prediction and Assessment, Padua, Italy, 14–17 June, 2011.
Schürch, P., Densmore, A. L., Rosser, N. J., Lim, M., and McArdell, B. W.: Detection of surface change in complex topography using terrestrial laser scanning: application to the Illgraben debris-flow channel, Earth Surf. Proc. Land., 36, 1847–1859, 2011a.
Schürch, P., Densmore, A. L., Rosser, N. J., and McArdell, B. W.: Dynamic controls on erosion and deposition on debris-flow fans, Geology, 39, 827–830, 2011b.
Sovilla, B., Burlando, P., and Bartelt, P.: Field experiments and numerical modelling of mass entrainment in snow avalanches, J. Geophys. Res., 111, 16 pp., F03007, doi:10.1029/2005JF000391, 2006.
Tobler, D., Kull, I., Jacquemart, M., and Haehlen, N.: Hazard management in a debris flow affected area: case study from Spreitgraben, Switzerland, Landslide Science for a Safer Geoenvironment, 3, 25–30, doi:10.1007/978-3-319-04996-0_5, 2014.

NHESSD
3, 2379–2417, 2015

Table 1. Data available for the erosion (modelling) analysis for the Spreitgraben (Geotest AG, 2012).The erosion depth and digital elevation models (DTM) provide the basis for the elevation change data sets.

Data set	Spreitgraben 2010		
debris flow events	12 Jul 2010 16 Jul 2010 21 Jul 2010	23 Jul 2010	12 Aug 2010
estimated event volumes [m^3]	3 × ≈ 10 000	≈ 90 000	≈ 130 000
flow height/discharge data	estimated using videos[(1)]		
erosion data	field observations[(1)]		
elevation data available for erosion analysis	LiDAR-based digital terrain models DTM[(2)] 04/2010 (cell size = 2 m) and 08/2010 (cell size = 1 m)		

[(1)] Geotest AG (2010–2012); [(2)] Cantonal authorities, Bern, Switzerland (2010).

NHESSD
3, 2379–2417, 2015

Table 2. Best-fit friction coefficients for the RAMMS debris-flow model (Voellmy friction relation, Eq. 4) with entrainment (Eq. 6) at the Illgraben for the 1 July 2008 debris flow (Berger et al., 2011).

	Input Parameters			Results				
	ξ^a [m s^{-2}]	μ^b []	ρ^c [kg m^{-1}]	t_t^d [s]	Q_p^e [m^3 s^{-1}]	h_{max}^f [m]	v_{max}^g [m^2 s^{-1}]	e_r^h [m]
observed	–	–	2.000	88	≈ 90	2.35	5.5	0.05–0.30
modelled	1.200	0.05	2.000	95	85–100	2.2–2.4	5.1–5.8	0.04–0.28

[a] Dry-Coulomb friction μ.
[b] Viscous-turbulent friction ξ.
[c] Bulk density ρ.
[d] Travel time t_t [s] between check dams 27 and 29.
[e] Peak discharge Q_p [m^3 s^{-1}].
[f] Maximum flow height h_{max} [m] at check dam 29.
[g] Maximum flow velocity v_{max} [m^2 s^{-1}] at the erosion sensor site (Berger et al., 2011).
[h] Net erosion range e_r [m] at the erosion sensor site (Berger et al., 2011).

NHESSD
3, 2379–2417, 2015

Table 3. The two largest debris flow events from 2010 are described by a two-surge input hydrograph used for the runout erosion model testing. Peak discharge Q_p (bold) is derived from debris flow event volumes V (bold) based on Eq. 7.

debris flow event	**RAMMS hydrograph point**	**time t** [s] after front arrival	**discharge Q_t** [$m^3 s^{-1}$] at time t	**volume V_t** [m^3] at time t
23 Jul 2010	1	0	0	0
	2	5	**755**	1.888
	3	30	465	17 138
	4	150	0	**45 038**
12 Aug 2010	1	0	0	0
	2	5	**1025**	2.562
	3	30	685	23 937
	4	150	0	**65 037**
total 2010				**110 075**

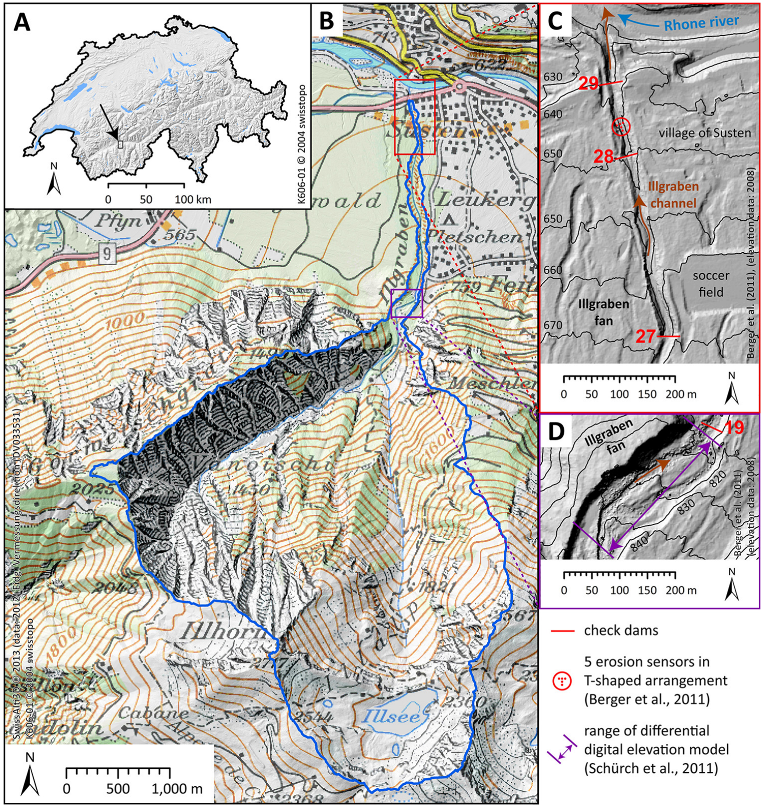

Figure 1. (a) The Illgraben catchment in Southern Switzerland **(b)** Locations of the instrumentation site and data available for the erosion analysis at the Illgraben catchment **(c)** On the lower fan of Illgraben, the location of the erosion sensors (Berger et al., 2011) and main instrumentation site (McArdell et al., 2007) on check dam 29 is shown. **(d)** The channel reach covered by the terrestrial laser scanning-based elevation-change analysis (Schürch et al., 2011b) is located on the upper fan below the fan apex.

NHESSD
3, 2379–2417, 2015

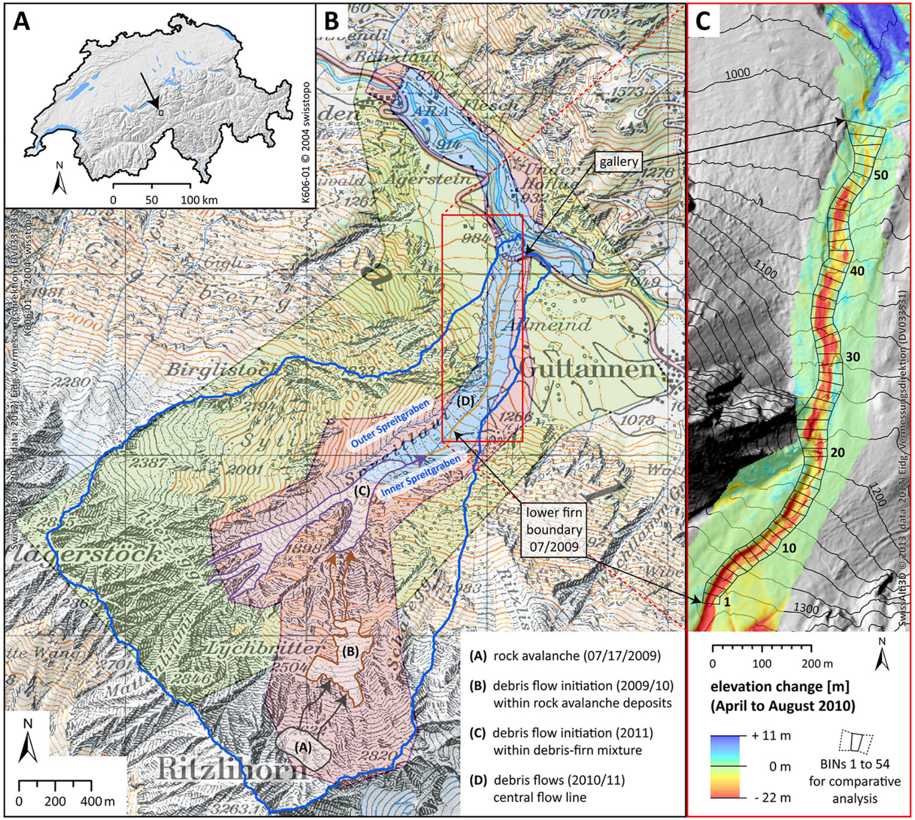

Figure 2. (a) The Spreitgraben catchment in Central Switzerland. **(b)** The processes observed in the catchment **(a)** to **(d)** during the most active years 2009 to 2011 and the coverage of the three available LiDAR-based digital terrain models DTM (2010 and 2011) for the erosion analysis: 04/2010 (raster cell: 2 m, blue polygon); 08/2010 (raster cell: 1 m, red polygon); 10/2011 (raster cell: 1 m, green polygon). **(c)** The elevation change (04/2010 to 08/2010) on the middle and lower fan are compared to erosion modelling results using bins numbered 1 to 54.

NHESSD
3, 2379–2417, 2015

Title Page
Abstract | Introduction
Conclusions | References
Tables | Figures
◀| |▶
◀ ▶
Back | Close
Full Screen / Esc
Printer-friendly Version
Interactive Discussion

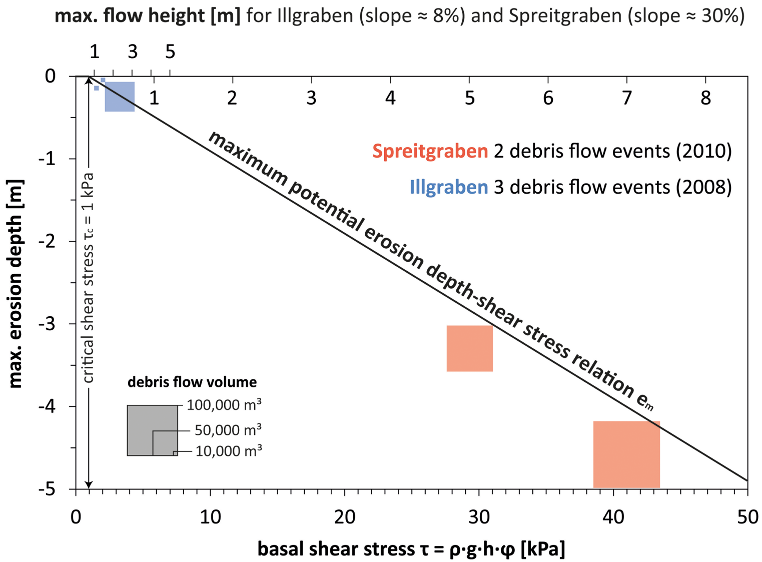

Figure 3. A linear relationship for maximum erosion depth as a function of basal shear stress forms the basis of the model. The size of the boxes is proportional to the estimated event volume at the Illgraben (3 debris-flow events, Berger et al., 2010) and Spreitgraben (2 events, Geotest AG, 2010). The upper axis indicates the flow height at the Illgraben (8 % channel slope) with the numbers above the axis, and at the Spreitgraben (30 % slope) with the flow depth values placed below the axis; the corresponding shear stresses (Eq. 5) are plotted at the bottom of the figure.

NHESSD
3, 2379–2417, 2015

Title Page
Abstract | Introduction
Conclusions | References
Tables | Figures
◀| |▶
◀ ▶
Back | Close
Full Screen / Esc
Printer-friendly Version
Interactive Discussion

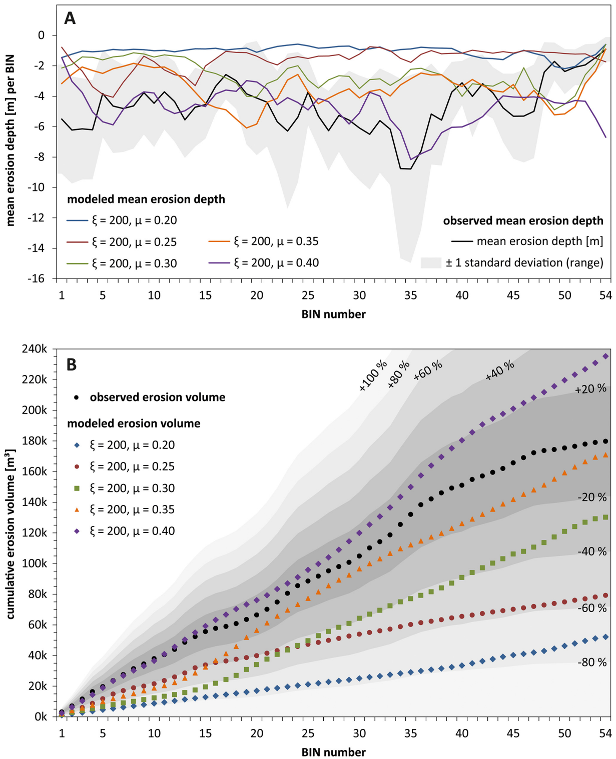

Figure 4. **(a)** Range of modelled compared to observed mean erosion depths. **(b)**. Modelled cumulative erosion volumes compared to observed cumulative erosion volumes using the bin-based systematic analysis. The gray shaded areas depict the ranges of percental volume difference compared with the observed erosion volume.

NHESSD
3, 2379–2417, 2015

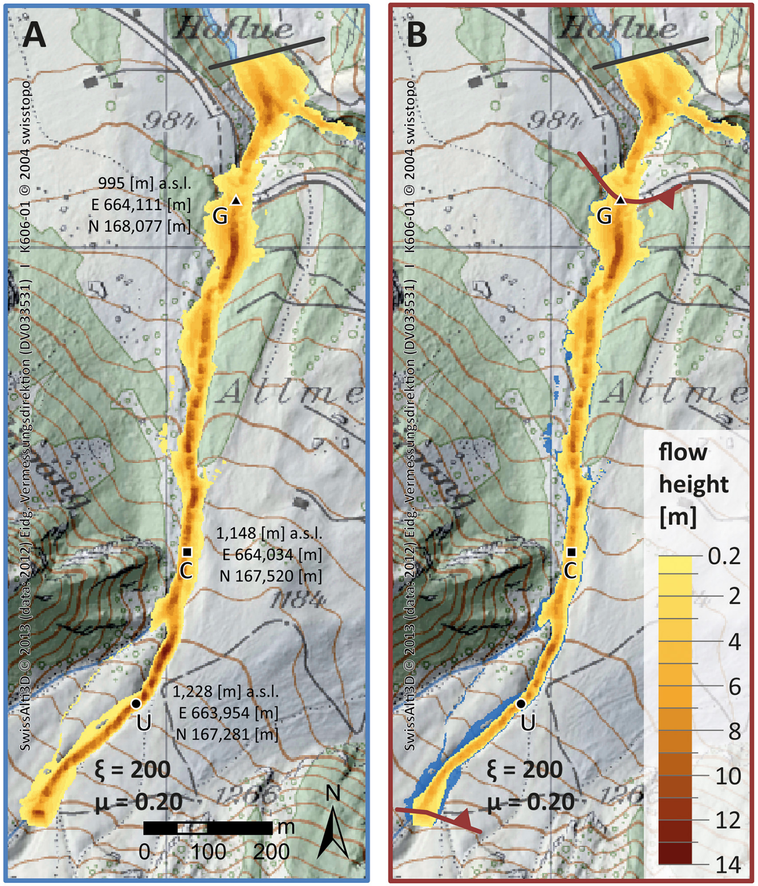

Figure 5. Maximum modelled flow height using no-erosion modelling **(a)** compared to erosion modelling **(b)**, showing considerable differences in the extent of over-bank flow (**(b)**: blue area). Locations U (upper fan, Inner Spreitgraben), C (below the confluence) and G (top of the road gallery) are used in Fig. 6.

NHESSD
3, 2379–2417, 2015

The importance of erosion for debris flow runout modelling

F. Frank et al.

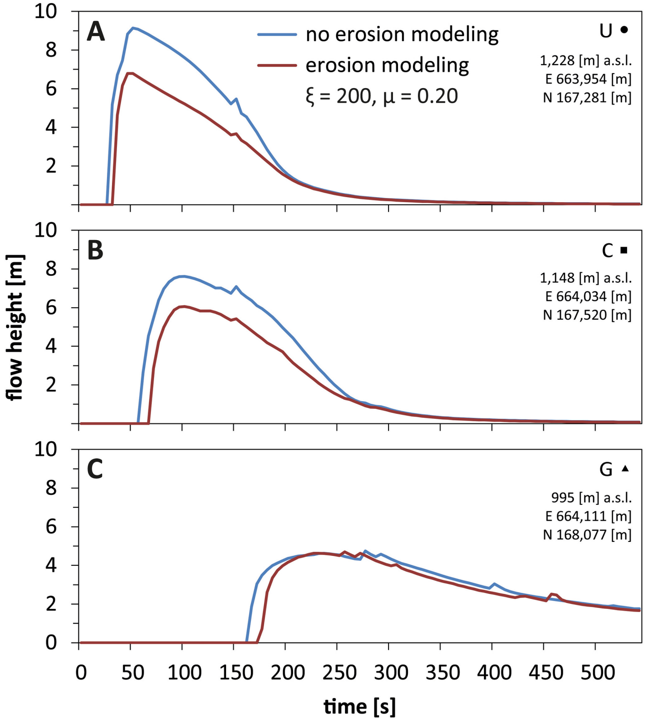

Figure 6. Comparison of modelled flow height using no-erosion modelling (blue lines) and erosion modelling (red lines) with distance along the channel. The different modelling locations (U, C, G) are shown in Fig. 5.

NHESSD
3, 2379–2417, 2015

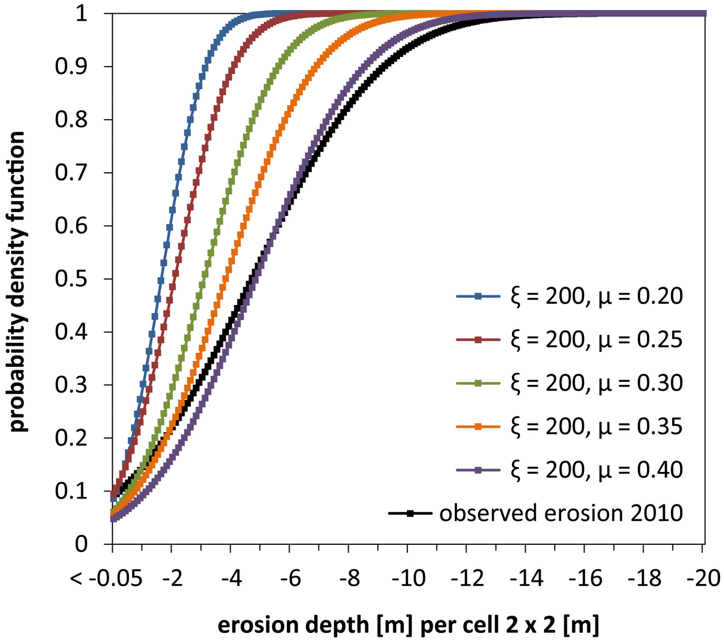

Figure 7. Probability-density plot of modelled vs. observed erosion depths based on a grid resolution of 2 m by 2 m in bins 1 to 54, for a total of 12 621 cells, using the DTMs of April 2010 and August 2010. Cells without erosion are not included.

NHESSD
3, 2379–2417, 2015

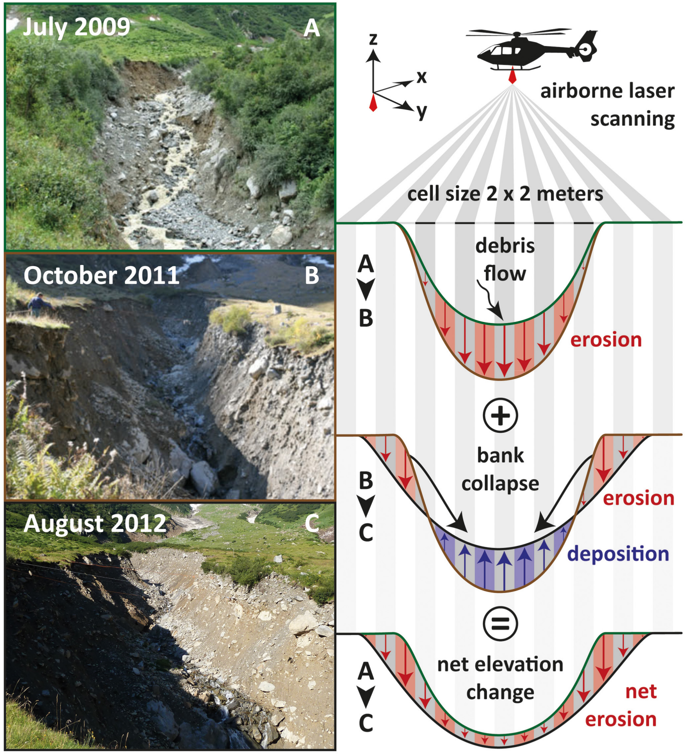

Figure 8. Conceptual model for the evolution of the debris-flow channel, in three stages, at the Spreitgraben during the three active years after the re-activation of the channel following the first large debris flow July 2009 (Photos: Geotest, 2009 and 2011; F. Frank, 2012). Several reiterations showing primary erosion (**a** to **b**) by debris flow degradation and secondary erosion (**b** to **c**) composed of lateral bank-collapses result in channel degradation and widening while channel bed is often composed of fresh and easily-erodible sediment deposits. Shaded columns are indicating observed erosion and deposition volume per cell. Arrows represent the mean erosion and deposition depths measured.